

Study of the p-p-K⁺ and p-p-K⁻ dynamics using the femtoscopy technique

(ALICE Collaboration) Acharya, S.; ...; Erhardt, Filip; ...; Gotovac, Sven; ...; Jerčić, Marko; ...; Karatović, David; ...; ...

Source / Izvornik: **The European Physical Journal A, 2023, 59**

Journal article, Published version

Rad u časopisu, Objavljena verzija rada (izdavačev PDF)

<https://doi.org/10.1140/epja/s10050-023-01139-9>

Permanent link / Trajna poveznica: <https://urn.nsk.hr/urn:nbn:hr:217:655177>

Rights / Prava: [Attribution 4.0 International](#)/[Imenovanje 4.0 međunarodna](#)

Download date / Datum preuzimanja: **2024-07-17**



Repository / Repozitorij:

[Repository of the Faculty of Science - University of Zagreb](#)





Study of the p - p - K^+ and p - p - K^- dynamics using the femtoscopy technique

ALICE Collaboration*

CERN, 1211 Geneva 23, Switzerland

Received: 28 April 2023 / Accepted: 21 September 2023 / Published online: 18 December 2023

© CERN for the benefit of the ALICE Collaboration 2023

Communicated by Frank Maas.

Abstract The interactions of kaons (K) and antikaons (\bar{K}) with few nucleons (N) were studied so far using kaonic atom data and measurements of kaon production and interaction yields in nuclei. Some details of the three-body KNN and $\bar{K}NN$ dynamics are still not well understood, mainly due to the overlap with multi-nucleon interactions in nuclei. An alternative method to probe the dynamics of three-body systems with kaons is to study the final state interaction within triplet of particles emitted in pp collisions at the Large Hadron Collider, which are free from effects due to the presence of bound nucleons. This Letter reports the first femtoscopic study of p - p - K^+ and p - p - K^- correlations measured in high-multiplicity pp collisions at $\sqrt{s} = 13$ TeV by the ALICE Collaboration. The analysis shows that the measured p - p - K^+ and p - p - K^- correlation functions can be interpreted in terms of pairwise interactions in the triplets, indicating that the dynamics of such systems is dominated by the two-body interactions without significant contributions from three-body effects or bound states.

The nature of kaons and antikaons is closely related to the chiral symmetry breaking pattern of low-energy QCD [1, 2]. Therefore, the study of kaon properties and their modification in dense nuclear matter has received the attention of the scientific community in the past decades. In particular, the hadronic interactions of charged kaons, K^+ and K^- , with nucleons (N) were investigated using kaonic atoms [3–5] and by studying the interaction or the production of kaons in light [6–14] and heavy nuclei [15–23]. Such measurements demonstrated the repulsive and attractive nature of the K^+N and K^-N strong interactions [1, 2], respectively. Information on the in-medium modification of the K^+ and K^- potentials with the increasing baryon density was extracted from the comparison of kaon production yields and flow observables measured in nucleus–nucleus collisions [15–17] and pion- and proton-induced reactions [18–23] with the expectations from transport models. Several K^+ nuclear poten-

tials have been tested and the best agreement with the data results in a repulsive strength of 20–40 MeV at nuclear saturation density. On the other hand, the K^-N interaction is known to be sufficiently attractive in the isospin $I = 0$ channel to dynamically generate the $\Lambda(1405)$ just below the K^-p threshold [24]. Such a state is interpreted as a quasi-bound antikaon–nucleon $\bar{K}N$ system which couples strongly to the $\pi\Sigma$ channel, giving rise to a sizable K^- absorption [25]. In the case of K^- nuclear interaction, the influence of single- and multi-nucleon absorption processes in nuclei currently prevents extracting firm conclusions on the strength of the K^- in-medium attractive potential [1]. This ambiguity triggered a longstanding debate in the literature about the possible existence of exotic kaonic bound objects with nucleons (see [1] and references therein). Recently, the E15 Collaboration reported the first experimental evidence of the $\bar{K}NN$ state with a binding energy of about 42 MeV and a decay width of about 100 MeV [26]. From the theoretical side, binding energies in the range 9–95 MeV and decay widths between 16 and 110 MeV are expected [27–42]. The uncertainties in the models mainly arise from scarce knowledge of the full $\bar{K}NN$ three-body effects, such as three-body coupled channels and two-nucleon absorption processes. Additionally, three-body forces, which are relevant in the calculation of the nuclear binding energies [43, 44], are currently not included in kaonic bound state models. Further experimental investigations on the K^+NN and K^-NN three-body dynamics, in addition to the studies of K^+ and K^- interaction in nuclei, are required to isolate and quantify the contribution from genuine three-body effects in such systems.

An alternative method to explore the three-body dynamics of K^+ and K^- with nucleons is to employ the femtoscopy technique at high-energy collider facilities. In small colliding systems, such as pp and p - Pb at the Large Hadron Collider (LHC), the inter-hadron distances at the time of the particle emission range from a few femtometers down to scales compatible with the nucleon size. This leads to an enhancement of the strength of the signal due to the

* e-mail: alice-publications@cern.ch

short-range strong interaction in the measured correlation function [45]. The femtoscopy method was proven to be able to test and constrain the hadron–hadron interaction for various two-particle systems [46–57], providing data with unprecedented precision on the hadronic interactions with strangeness at low relative momenta, down to the energy threshold of the produced pairs. Furthermore, the measured femtoscopic correlation functions are sensitive to the presence of bound states in the energy region below the threshold. Thus, they were also used to constrain the parameters of bound hadron–hadron systems [49, 58]. Recently, the ALICE Collaboration has extended the method to explore the correlation among three baryons, such as p – p – p and p – p – Λ , to study the dynamics of three-body systems [59]. The analysis exploited Kubo’s cumulant expansion method [60] and the projector method [61] to isolate the genuine three-particle correlations from the measured correlation functions. As a result, a first experimental hint of genuine three-body effects in the unbound p – p – p system was found. The study in this Letter applies the same analysis procedure adopted in [59] to the case of p – p – K^+ and p – p – K^- particle triplets to explore possible genuine three-body effects in the correlation functions induced by the strong interaction and bound state formation. The main advantage of the femtoscopy method with respect to the previous experimental techniques is the possibility to investigate for the first time the K^+ and K^- three-body dynamics with nucleons, free from additional effects induced by the presence of the surrounding nucleons in nuclei.

The analysed data sample of pp collisions at $\sqrt{s} = 13$ TeV was recorded by ALICE [62–64] during the LHC Run 2 (2015–2018) data-taking period. In the following, the information from the V0 detector system [65], the inner tracking system (ITS) [66], the time projection chamber (TPC) [67] and the time-of-flight (TOF) detector [68] is used. The V0 detector is employed to trigger on high-multiplicity (HM) events. This trigger selects events within the 0.17% largest charged-track multiplicity of the $INEL > 0$ class, which is defined as inelastic collisions with at least one measured charged particle in the pseudorapidity range $|\eta| < 1$ [65]. This condition results in an average of about 30 charged particles in the range $|\eta| < 0.5$ [51], hence increasing the probability of finding triplets of the desired particle species with respect to the minimum-bias sample. The primary vertex position is reconstructed with the combined information of the ITS and the TPC, and, independently, with track segments in the two innermost layers of the ITS. Only events with a reconstructed primary vertex position along the beam axis within 10 cm from the centre of the ALICE detector are selected. A total of 10^9 HM events are used in this analysis. The p – p – K^+ and p – p – K^- data samples are built by combining three charged-particle tracks (triplets) reconstructed with the TPC. Assuming the same interactions in the particle

and antiparticle systems, triplets of particles and the corresponding antiparticles are combined: p – p – $K^+ \equiv (p$ – p – $K^+ \oplus \bar{p}$ – \bar{p} – $K^-)$ and p – p – $K^- \equiv (p$ – p – $K^- \oplus \bar{p}$ – \bar{p} – $K^+)$. The agreement of the corresponding correlation functions confirmed the validity of this assumption.

Particles and antiparticles are identified using the same kinematic and topological selections. Protons and kaons are selected in the range $|\eta| < 0.8$ and in the transverse momentum intervals $p_T \in (0.5$ – $4.05)$ GeV/ c and $p_T \in (0.2$ – $2.5)$ GeV/ c , respectively. A minimum of 80 space points (hits) inside the TPC, out of the total 159, is required to guarantee track quality and good momentum resolution. Particle identification (PID) is conducted by requiring that the measured energy loss (dE/dx) in the TPC gas is compatible with the expected one from protons and kaons within three standard deviations (σ). For high momentum particles, the dE/dx information is combined with the time-of-flight measurement provided by the TOF, using a 3σ selection on the expected value for a given particle hypothesis at a given momentum. The PID selection for protons is described in detail in [46]. The selection of kaons is based on the procedure described in [54] with several changes as explained in the following. TPC reconstructed tracks are identified as kaons either by using TPC PID information for momenta lower than 0.85 GeV/ c , or, if a signal in the TOF is matched to the TPC track, by using the combined PID information from TPC and TOF up to a momentum of 2.5 GeV/ c . To improve the purity of the kaon selection, the TPC and TOF information are also used to reject candidates that are compatible with the pion or electron hypothesis. To reject particles that are non-primary or come from pile-up collisions, the distance of closest approach (DCA) to the primary vertex of the tracks is required to be less than 0.1 cm in the transverse plane and less than 0.2 cm along the beam axis. The purity of the proton and kaon candidates is estimated employing Monte Carlo simulations based on PYTHIA 8 [69] (Monash 2013 Tune) event generator with a dedicated high-multiplicity selection to mimic the V0 high-multiplicity trigger and the GEANT4 package [70, 71]. The purity averaged over the p_T ranges of the identified protons and kaons is about 98% for both particle species.

The number of selected and analysed triplets amounts to 4530 for p – p – K^+ , 3161 for \bar{p} – \bar{p} – K^- , 6200 for p – p – K^- and 4937 for \bar{p} – \bar{p} – K^+ in the femtoscopic region $Q_3 < 0.4$ GeV/ c . The kinematic variable Q_3 , which is used in three-body analyses [59, 72], is a Lorentz-invariant scalar defined as $Q_3 = \sqrt{-q_{12}^2 - q_{23}^2 - q_{31}^2}$, where q_{ij} is the norm of the relative four-momentum of the pair ij in the triplet $q_{ij}^\mu = 2 [m_j/(m_i + m_j) p_i^\mu - m_i/(m_i + m_j) p_j^\mu]$. The systematic uncertainties of the correlation functions are evaluated by performing simultaneous variations of the selection criteria for particles and antiparticles. For protons and

antiprotons, the same variations for the track selection and PID criteria as in [59] are performed. Similar variations are used for the kaons and antikaons. In order to account for the correlations between the systematic uncertainties, the variations are randomly combined in sets in which at least one selection criterion is changed. Large statistical fluctuations introduced by the variations of the selection criteria are avoided by requiring that the yield of the triplets changes by less than 10% with respect to the standard selection in the femtoscopic region $Q_3 < 0.4 \text{ GeV}/c$. The main contribution at low Q_3 ($\approx 0.15 \text{ GeV}/c$) is given by the variation of the DCA selection and it is found to be smaller than 5%.

The final state interactions (FSIs) among the hadrons emitted in the collisions can be explored using correlation functions [73,74] in momentum space, defined as

$$C_3(\mathbf{p}_1, \mathbf{p}_2, \mathbf{p}_3) = \frac{P_3(\mathbf{p}_1, \mathbf{p}_2, \mathbf{p}_3)}{P_1(\mathbf{p}_1)P_1(\mathbf{p}_2)P_1(\mathbf{p}_3)}, \tag{1}$$

where \mathbf{p}_i is the momentum vector of the i -th particle and $P_3(\mathbf{p}_1, \mathbf{p}_2, \mathbf{p}_3)$ and $P_1(\mathbf{p}_i)$ are the probabilities of finding three particles and one particle with the corresponding momentum, respectively. If the particles are not correlated $P_3(\mathbf{p}_1, \mathbf{p}_2, \mathbf{p}_3) = P_1(\mathbf{p}_1)P_1(\mathbf{p}_2)P_1(\mathbf{p}_3)$ and then the correlation function becomes identical to unity. The presence of FSIs induces a correlation signal imprinted in the correlation function which causes deviations from unity depending on the nature of the interactions, attractive or repulsive, as well as on the properties of the emitting source (see [45,75] for the details). In the case of three-particle systems, the correlation function can be evaluated in terms of Q_3 . Hence, three-particle correlation functions are experimentally obtained as

$$C_3(Q_3) = \mathcal{N} \frac{N_{\text{same}}(Q_3)}{N_{\text{mixed}}(Q_3)}, \tag{2}$$

where \mathcal{N} is a normalisation parameter, $N_{\text{same}}(Q_3)$ is the Q_3 distribution of the particle triplets emitted in the same collision and $N_{\text{mixed}}(Q_3)$ is the distribution of uncorrelated triplets. The latter are obtained by taking the three particles needed to form a triplet from three different collisions, thus called mixed event sample. Only events with similar multiplicity and position of the primary vertex along the beam axis are mixed. The number of events used for the mixing is set to 30. To account for the two-track merging and splitting effects due to the finite two-track resolution in the same event sample, a minimum value of the distance between the same charge tracks on the azimuthal–polar angle plane $\Delta\eta$ – $\Delta\varphi$ is applied to both the same and mixed event samples. The default selection is $\Delta\eta^2 + \Delta\varphi^2 \geq (0.017)^2$ for p–p tracks and $\Delta\eta^2/(0.012)^2 + \Delta\varphi^2/(0.04)^2 \geq 1$ for p–K⁺ tracks. A systematic variation of about +10% for the values of the minimum distance is applied in the analysis. The correlation

function is normalised to unity in the range $1.0 < Q_3 < 1.2 \text{ GeV}/c$, where no signal from FSIs is expected. Variations of the normalisation range are performed and included in the systematic uncertainties. In the case of a particle triplet X–Y–Z, pairwise correlations with one uncorrelated particle (X–Y)–Z, X–(Y–Z) and (Z–X)–Y also occur in the system. Genuine three-particle correlations were isolated in [59] by applying the cumulant expansion method to the femtoscopic correlation functions. The three-particle cumulant $c_3(Q_3)$, which incorporates information about the three-body effects in the system, is computed from the measured correlation function $C_3(Q_3)$ as follows

$$c_3(Q_3) = C_3(Q_3) - C_{\text{two-body}}(Q_3), \tag{3}$$

where pairwise correlations are evaluated following the cumulant decomposition as

$$C_{\text{two-body}}(Q_3) = C_{(X-Y)-Z}(Q_3) + C_{X-(Y-Z)}(Q_3) + C_{(Z-X)-Y}(Q_3) - 2. \tag{4}$$

Each component $C_{(i-j)-k}(Q_3)$ of the lower-order contributions in Eq. (4) is computed using two methods [59,61]: (i) a data-driven approach based on the event mixing technique, building triplets in which the correlated (i–j) pairs are emitted in the same collision and the uncorrelated particle –k from another collision; (ii) the projector method which uses as input the measured two-particle correlation function $C(k^*)$ for the correlated pair (i–j), evaluated in terms of the relative momentum k^* in the pair rest frame (PRF), and calculates all the possible k^* configurations in the phase space for each Q_3 value of the i–j–k triplet. The input correlation functions $C(k^*)$ used in the projector method are obtained by selecting p–p, p–K⁺ and p–K[–] pairs using the same dataset as for the three-body analysis. Unlike the p–p and p–K⁺ pairs, the p–K[–] correlation is significantly affected by the contribution from jet-like events [76]. To use particles emitted in collisions with the same event shape as in the case of the analysed triplets, p–K[–] pairs are selected from p–p–K[–] triplets with $Q_3 < 1 \text{ GeV}/c$, while for p–p and p–K⁺ pairs such additional requirement is not used as the correlation functions with and without the Q_3 selection are in agreement. A $\pm 0.1 \text{ GeV}/c$ variation of the Q_3 limit is included in the systematic uncertainties of the projector method and it is combined with the uncertainties propagated from the data points of the p–p, p–K⁺ and p–K[–] correlation functions. The latter include the variations in the selection criteria for particles, variations in the track splitting/merging rejection criteria, and normalisation range.

For the p–p–K⁺ and p–p–K[–] systems, the lower-order contributions to the three-particle correlation functions are shown in Fig. 1, using the data-driven approach (data points) and the projector method (grey bands). The three-particle

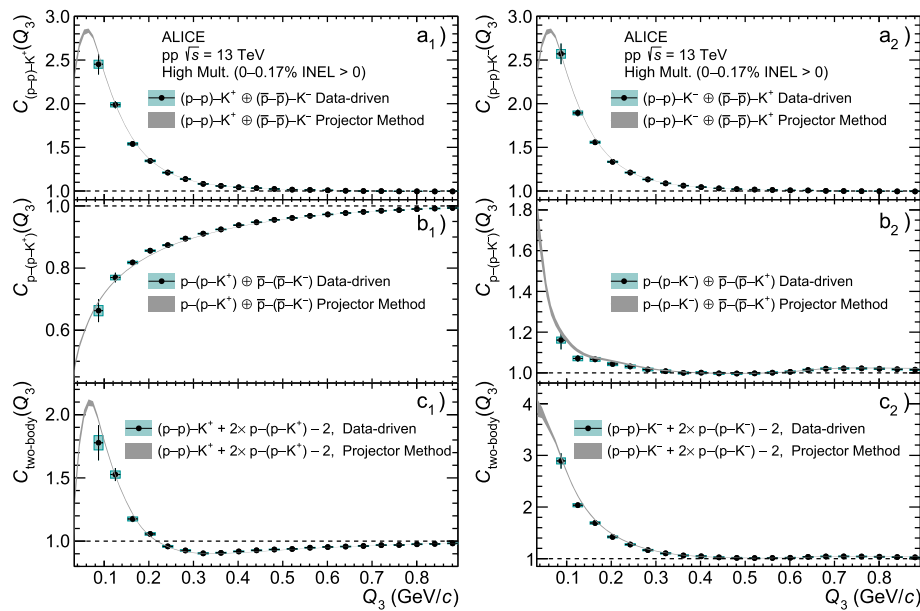


Fig. 1 Correlation functions for $(p-p)-K^+$ (a₁), $(p-p)-K^-$ (a₂), $p-(p-K^+)$ (b₁), $p-(p-K^-)$ (b₂) as well as the total lower-order contributions for $p-p-K^+$ (c₁) and $p-p-K^-$ (c₂) as a function of Q_3 . The points represent the results obtained using the data-driven approach, with the

statistical and systematic uncertainties represented by the error bars and the green boxes, respectively. The grey bands are the expectations of the projector method, with the band width representing the combined statistical and systematic uncertainties

correlation functions of two correlated protons and an uncorrelated kaon, denoted as $(p-p)-K^+$ and $(p-p)-K^-$, are shown in panels (a₁) and (a₂), respectively. In both cases, the correlation functions are larger than unity in the low Q_3 region as a result of the attractive $p-p$ strong interaction, combined with the repulsive Coulomb and quantum statistics effects (see [46,48] for more details). In the case of correlated $p-K^+$ pairs with uncorrelated protons, $p-(p-K^+)$, the correlation function shown in panel (b₁) is lower than unity as a result of the repulsive $p-K^+$ strong and Coulomb interactions, consistent with the measurement reported in [47]. In the $p-(p-K^-)$ correlation function, shown in panel (b₂), the main features of the $p-K^-$ interaction are visible [47]: the cusp structure due to the opening of the \bar{K}^0 n channel as well as the bump due to the $\Lambda(1520) \rightarrow pK^-$ decay appear at $Q_3 \approx 0.15$ GeV/c and $Q_3 \approx 0.7$ GeV/c, respectively. The total lower-order contributions to the $p-p-K^+$, panel (c₁), and $p-p-K^-$, panel (c₂), correlation functions evaluated with the data-driven approach and the projector method are in agreement. The reduced χ^2 between the two methods, evaluated in the Q_3 range shown in Fig. 1 (21 degrees of freedom) by adding in quadrature the statistical and systematic uncertainties of the data, is 1.6 and 1.4 for $p-p-K^+$ and $p-p-K^-$, respectively. Since the projector method does not depend on the third particle mixing, it provides significantly smaller uncertainties than the data-driven approach and hence is used to extract the cumulants. This choice does not affect the final results of the analysis. Figure 2 shows the measured $p-p-K^+$ (left panel) and $p-p-K^-$ (right panel) correlation functions

(data points) compared to the lower-order contributions evaluated using the projector method (grey bands).

The corresponding cumulants are extracted using Eq. (3). The measured cumulants include the correlations of the primary particles as well as the feed-down from resonances and particle misidentifications, which need to be accounted for as discussed in [59]. The number of correctly identified primary triplets is about 66% of the total sample for both $p-p-K^+$ and $p-p-K^-$. The remaining contribution mainly stems from the feed-down of the Λ (17%) and Σ^+ (7%) hyperon decays into protons and from the ϕ meson (4%) decay into charged kaons. These numbers are obtained combining the primary and secondary fractions with particle purities. The primary and secondary fractions are extracted using Monte Carlo template fits to the measured distributions of the DCA to the primary vertex [46]. The fraction of charged kaons from ϕ decays is calculated using the expectations from a thermal model [77]. The correction of the measured cumulants to obtain the contribution from primary triplets is performed following the decomposition procedure adopted in [59]. Due to the absence of theoretical and experimental information on the genuine $p-\Lambda-K^\pm$, $p-\Sigma^+-K^\pm$ and $p-p-\phi$ correlations, the corresponding feed-down contributions to the $p-p-K^\pm$ cumulants are considered to be flat, without any specific dependence on Q_3 . This assumption was tested in the case of $p-p-p$ correlations [59], where a similar contribution (about 19%) for the Λ feed-down into protons was found. The results obtained by using the flat and non-flat corrections are found to be in agreement within the uncertainties. A flat feed-

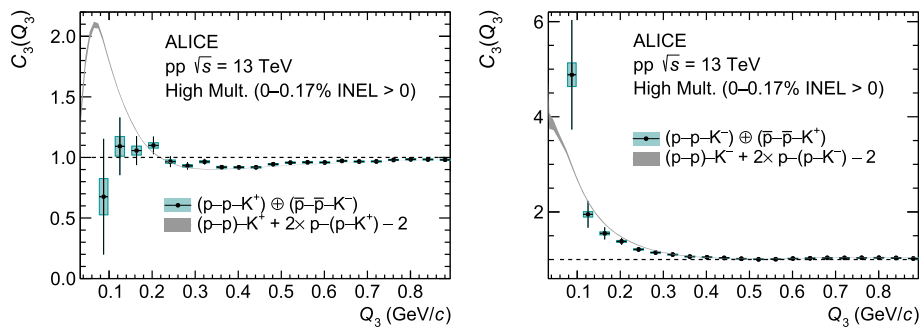


Fig. 2 Correlation functions (data points) for p–p–K⁺ (left panel) and p–p–K[−] (right panel) compared to the lower-order contributions evaluated using the projector method (grey bands). Statistical and systematic uncertainties are represented by error bars and green boxes, respectively.

The band widths represent the combined statistical and systematic uncertainties propagated from the two-particle correlation functions used as input to the projector method

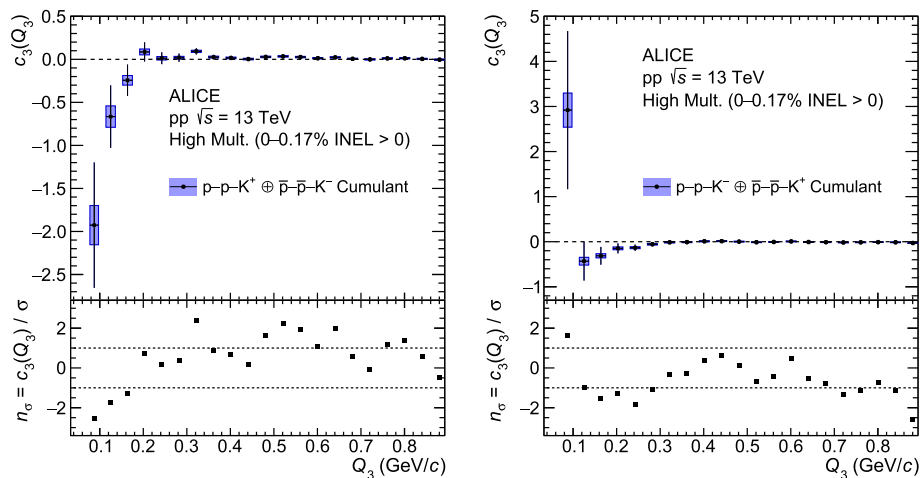


Fig. 3 Cumulants for the p–p–K⁺ (left panel) and p–p–K[−] (right panel) primary triplets. The error bars and the blue boxes on the data points represent the statistical and systematic uncertainties, respectively.

The n_σ deviations from zero in each bin are shown in the bottom panels, adding in quadrature the statistical and systematic uncertainties of the data

down contribution in the cumulant corresponds to negligible correlations from genuine three-body effects in the mother particle systems X–Y–Z decaying into p–p–K[±]. The dominant feed-down contributions coming from pairwise correlations in the triplets, such as (X–Y)–Z and X–(Y–Z), are already removed as they are included in the lower-order correlations. The resulting cumulants of the correctly identified primary p–p–K⁺ and p–p–K[−] particle triplets are shown in left and right panels of Fig. 3, respectively.

In the absence of genuine three-particle correlations in the triplets, the measured three-particle correlation function would be identical to the lower-order contributions $C_3(Q_3) = C_{\text{two-body}}(Q_3)$. Consequently, from Eq. (3), the cumulant would be compatible with zero within the experimental uncertainties. In the case of the p–p–K⁺ and p–p–K[−] systems, the agreement of the measured cumulants with zero is evaluated by performing a χ^2 test in the region $Q_3 < 0.4$ GeV/c. In this region, the relative momentum for all the

pairs in the particle triplets is lower than 0.2 GeV/c, which is the kinematic region sensitive to the strong interaction. Larger Q_3 values are dominated by kinematic configurations in which one of the pairs has a relative momentum larger than 0.2 GeV/c, meaning that only two of the three particles in the triplet can be in a kinematic configuration which is favourable for the strong interaction. Thus, at $Q_3 > 0.4$ GeV/c the contributions from the two-body interaction dominate. The local statistical significance at $Q_3 < 0.4$ GeV/c is obtained from the p-value of the χ^2 distribution, which is converted in a number n_σ of Gaussian standard deviations. As the systematic uncertainties in different Q_3 bins are correlated, the χ^2 is calculated using the cumulants extracted from each systematic variation with the corresponding statistical uncertainties. Finally, the average χ^2 in the interval $Q_3 < 0.4$ GeV/c is extracted. The corresponding n_σ values are 2.5 and 1.5 for p–p–K⁺ and p–p–K[−], respectively. As the Q_3 range of the genuine three-body effects is not known

a priori, the n_σ values have been evaluated as well in the region $Q_3 < 0.2 \text{ GeV}/c$ and they are found to be 2.7 and 1.4 for $p\text{-}p\text{-}K^+$ and $p\text{-}p\text{-}K^-$, respectively. Such results indicate that the measured $p\text{-}p\text{-}K^+$ and $p\text{-}p\text{-}K^-$ correlation functions are compatible, within the quoted significance levels, with the assumption of pairwise correlations in the triplets without additional contributions from genuine three-body effects. More solid conclusions require a larger data sample to reduce the statistical uncertainties and full-fledged theoretical calculations for the three-particle correlation functions. In order to provide a comparison of the kinematic range accessible with this measurement to the study of K^+ and K^- interactions in light nuclei, the momenta of the three particles in the triplets with $Q_3 < 0.4 \text{ GeV}/c$ are evaluated in the PRF of the two protons. The momentum of each proton in the PRF is $p_p^* < 180 \text{ MeV}/c$, compatible with the typical Fermi momenta of nucleons in light nuclei (e.g. the Fermi momentum in Carbon-12 is about $220 \text{ MeV}/c$). In the rest frame of the two protons, the momentum of the K^+ and K^- ranges from $30 \text{ MeV}/c$ (in the first bin in Fig. 3) to $130 \text{ MeV}/c$ (eighth bin in Fig. 3). This demonstrates that even for low kaon momenta, i.e. at energies close to the $p\text{-}p\text{-}K^+$ and $p\text{-}p\text{-}K^-$ thresholds, three-body effects such as kaonic bound state formation below threshold or three-body interactions do not contribute significantly to the measured correlation functions. These results provide additional experimental information for theoretical models aiming to understand the role of genuine three-body effects in $p\text{-}p\text{-}K^+$ and $p\text{-}p\text{-}K^-$ systems. The LHC Run 3 data taking will deliver a larger data set for more detailed studies of the K^+ and K^- three-body dynamics in the low momentum region, down to the energy threshold of the triplets.

Acknowledgements The ALICE Collaboration would like to thank all its engineers and technicians for their invaluable contributions to the construction of the experiment and the CERN accelerator teams for the outstanding performance of the LHC complex. The ALICE Collaboration gratefully acknowledges the resources and support provided by all Grid centres and the Worldwide LHC Computing Grid (WLCG) collaboration. The ALICE Collaboration acknowledges the following funding agencies for their support in building and running the ALICE detector: A. I. Alikhanyan National Science Laboratory (Yerevan Physics Institute) Foundation (ANSL), State Committee of Science and World Federation of Scientists (WFS), Armenia; Austrian Academy of Sciences, Austrian Science Fund (FWF): [M 2467-N36] and Nationalstiftung für Forschung, Technologie und Entwicklung, Austria; Ministry of Communications and High Technologies, National Nuclear Research Center, Azerbaijan; Conselho Nacional de Desenvolvimento Científico e Tecnológico (CNPq), Financiadora de Estudos e Projetos (Finep), Fundação de Amparo à Pesquisa do Estado de São Paulo (FAPESP) and Universidade Federal do Rio Grande do Sul (UFRGS), Brazil; Bulgarian Ministry of Education and Science, within the National Roadmap for Research Infrastructures 2020–2027 (object CERN), Bulgaria; Ministry of Education of China (MOEC), Ministry of Science & Technology of China (MSTC) and National

Natural Science Foundation of China (NSFC), China; Ministry of Science and Education and Croatian Science Foundation, Croatia; Centro de Aplicaciones Tecnológicas y Desarrollo Nuclear (CEADEN), Cubaenergía, Cuba; Ministry of Education, Youth and Sports of the Czech Republic, Czech Republic; The Danish Council for Independent Research | Natural Sciences, the VILLUM FONDEN and Danish National Research Foundation (DNRF), Denmark; Helsinki Institute of Physics (HIP), Finland; Commissariat à l’Energie Atomique (CEA) and Institut National de Physique Nucléaire et de Physique des Particules (IN2P3) and Centre National de la Recherche Scientifique (CNRS), France; Bundesministerium für Bildung und Forschung (BMBF) and GSI Helmholtzzentrum für Schwerionenforschung GmbH, Germany; General Secretariat for Research and Technology, Ministry of Education, Research and Religions, Greece; National Research, Development and Innovation Office, Hungary; Department of Atomic Energy Government of India (DAE), Department of Science and Technology, Government of India (DST), University Grants Commission, Government of India (UGC) and Council of Scientific and Industrial Research (CSIR), India; National Research and Innovation Agency - BRIN, Indonesia; Istituto Nazionale di Fisica Nucleare (INFN), Italy; Japanese Ministry of Education, Culture, Sports, Science and Technology (MEXT) and Japan Society for the Promotion of Science (JSPS) KAKENHI, Japan; Consejo Nacional de Ciencia (CONACYT) y Tecnología, through Fondo de Cooperación Internacional en Ciencia y Tecnología (FONCICYT) and Dirección General de Asuntos del Personal Académico (DGAPA), Mexico; Nederlandse Organisatie voor Wetenschappelijk Onderzoek (NWO), Netherlands; The Research Council of Norway, Norway; Commission on Science and Technology for Sustainable Development in the South (COMSATS), Pakistan; Pontificia Universidad Católica del Perú, Peru; Ministry of Education and Science, National Science Centre and WUT ID-UB, Poland; Korea Institute of Science and Technology Information and National Research Foundation of Korea (NRF), Republic of Korea; Ministry of Education and Scientific Research, Institute of Atomic Physics, Ministry of Research and Innovation and Institute of Atomic Physics and University Politehnica of Bucharest, Romania; Ministry of Education, Science, Research and Sport of the Slovak Republic, Slovakia; National Research Foundation of South Africa, South Africa; Swedish Research Council (VR) and Knut & Alice Wallenberg Foundation (KAW), Sweden; European Organization for Nuclear Research, Switzerland; Suranaree University of Technology (SUT), National Science and Technology Development Agency (NSTDA), Thailand Science Research and Innovation (TSRI) and National Science, Research and Innovation Fund (NSRF), Thailand; Turkish Energy, Nuclear and Mineral Research Agency (TENMAK), Turkey; National Academy of Sciences of Ukraine, Ukraine; Science and Technology Facilities Council (STFC), United Kingdom; National Science Foundation of the United States of America (NSF) and United States Department of Energy, Office of Nuclear Physics (DOE NP), United States of America. In addition, individual groups or members have received support from: European Research Council, Strong 2020 - Horizon 2020 (grant nos. 950692, 824093), European Union; Academy of Finland (Center of Excellence in Quark Matter) (grant nos. 346327, 346328), Finland; Programa de Apoyos para la Superación del Personal Académico, UNAM, Mexico.

Funding Open access funding provided by CERN (European Organization for Nuclear Research)

Data availability This manuscript has no associated data or the data will not be deposited. [Authors’ comment: Manuscript has associated data in a HEPData repository at <https://www.hepdata.net/record/ins2648608>.]

Open Access This article is licensed under a Creative Commons Attribution 4.0 International License, which permits use, sharing, adaptation, distribution and reproduction in any medium or format, as long as you

give appropriate credit to the original author(s) and the source, provide a link to the Creative Commons licence, and indicate if changes were made. The images or other third party material in this article are included in the article's Creative Commons licence, unless indicated otherwise in a credit line to the material. If material is not included in the article's Creative Commons licence and your intended use is not permitted by statutory regulation or exceeds the permitted use, you will need to obtain permission directly from the copyright holder. To view a copy of this licence, visit <http://creativecommons.org/licenses/by/4.0/>.

References

1. L. Tolos, L. Fabbietti, Strangeness in nuclei and neutron stars. *Prog. Part. Nucl. Phys.* **112**, 103770 (2020). <https://doi.org/10.1016/j.pnpnp.2020.103770>. arXiv:2002.09223 [nucl-ex]
2. T. Hyodo, W. Weise, Theory of kaon-nuclear systems, in *Handbook of Nuclear Physics*, eds. by H.T.I. Tanihata, T. Kajino, p. 2. Springer (2022). arXiv:2202.06181 [nucl-th]
3. C. Batty, E. Friedman, A. Gal, Strong interaction physics from hadronic atoms. *Phys. Rep.* **287**, 385–445 (1997). [https://doi.org/10.1016/S0370-1573\(97\)00011-2](https://doi.org/10.1016/S0370-1573(97)00011-2)
4. E. Friedman, A. Gal, K^-N amplitudes below threshold constrained by multinucleon absorption. *Nucl. Phys. A* **959**, 66–82 (2017). <https://doi.org/10.1016/j.nuclphysa.2016.12.009>. arXiv:1610.04004 [nucl-th]
5. C. Curceanu et al., The modern era of light kaonic atom experiments. *Rev. Mod. Phys.* **91**, 025006 (2019). <https://doi.org/10.1103/RevModPhys.91.025006>
6. P.A. Katz et al., Reactions of stopping K^- in helium. *Phys. Rev. D* **1**, 1267–1276 (1970). <https://doi.org/10.1103/PhysRevD.1.1267>
7. C. Vander Velde-Wilquet et al., Determination of the branching fractions for K^- meson absorption at rest in carbon nuclei. *Nuovo Cim.* **A39**, 538–547 (1977). <https://doi.org/10.1007/BF02771028>
8. R. Michael et al., K^+ elastic scattering from C and ${}^6\text{Li}$ at 715 MeV/c. *Phys. Lett. B* **382**, 29–34 (1996). [https://doi.org/10.1016/0370-2693\(96\)00664-8](https://doi.org/10.1016/0370-2693(96)00664-8)
9. FINUDA Collaboration, M. Agnello et al., Σ^-p emission rates in K^- absorptions at rest on ${}^6\text{Li}$, ${}^7\text{Li}$, ${}^9\text{Be}$, ${}^{13}\text{C}$, and ${}^{16}\text{O}$. *Phys. Rev. C* **92**, 045204 (2015). <https://doi.org/10.1103/PhysRevC.92.045204>. arXiv:1508.00139 [nucl-ex]
10. O. Vazquez Doce et al., K^- absorption on two nucleons and ppK^- bound state search in the Σ^0p final state. *Phys. Lett. B* **758**, 134–139 (2016). <https://doi.org/10.1016/j.physletb.2016.05.001>. arXiv:1511.04496 [nucl-ex]
11. K. Piscicchia et al., First measurement of the $K^-n \rightarrow \Lambda\pi^-$ non-resonant transition amplitude below threshold. *Phys. Lett. B* **782**, 339–345 (2018). <https://doi.org/10.1016/j.physletb.2018.05.025>
12. R. Del Grande et al., K^- multi-nucleon absorption cross sections and branching ratios in Λp and $\Sigma^0 p$ final states. *Eur. Phys. J. C* **79**, 1–13 (2019). <https://doi.org/10.1140/epjc/s10052-019-6694-7>. arXiv:1809.07212 [nucl-ex]
13. C.M. Kormanyos et al., Quasielastic K^+ scattering. *Phys. Rev. C* **51**, 669–679 (1995). <https://doi.org/10.1103/PhysRevC.51.669>
14. R. Weiss et al., Measurement of low energy K^+ total cross sections on $N=Z$ nuclei. *Phys. Rev. C* **49**, 2569–2577 (1994). <https://doi.org/10.1103/PhysRevC.49.2569>
15. FOPI Collaboration, P. Crochet et al., Sideward flow of K^+ mesons in Ru+Ru and Ni+Ni reactions near threshold. *Phys. Lett. B* **486**, 6–12 (2000). [https://doi.org/10.1016/S0370-2693\(00\)00712-7](https://doi.org/10.1016/S0370-2693(00)00712-7)
16. KaoS Collaboration, A. Förster et al., Production of K^+ and of K^- mesons in heavy-ion collisions from 0.6A to 2.0A GeV incident energy. *Phys. Rev. C* **75**, 024906 (2007). <https://doi.org/10.1103/PhysRevC.75.024906>
17. F.O.P.I. Collaboration, V. Zinyuk et al., Azimuthal emission patterns of K^+ and of K^- mesons in Ni + Ni collisions near the strangeness production threshold. *Phys. Rev. C* **90**, 025210 (2014). <https://doi.org/10.1103/PhysRevC.90.025210>
18. M. Büscher et al., Phenomenological analysis of K^+ -meson production in proton-nucleus collisions. *Phys. Rev. C* **65**, 014603 (2001). <https://doi.org/10.1103/PhysRevC.65.014603>
19. KaoS Collaboration, W. Scheinast et al., In-medium effects on phase space distributions of antikaons measured in proton-nucleus collisions. *Phys. Rev. Lett.* **96**, 072301 (2006). <https://doi.org/10.1103/PhysRevLett.96.072301>
20. HADES Collaboration, J. Adamczewski-Musch et al., Strong absorption of hadrons with hidden and open strangeness in nuclear matter. *Phys. Rev. Lett.* **123**, 022002 (2019). <https://doi.org/10.1103/PhysRevLett.123.022002>
21. A.N.K.E. Collaboration, M. Büscher et al., Inclusive K^\pm meson production in proton-nucleus interactions. *Eur. Phys. J. A* **22**, 301–317 (2004). <https://doi.org/10.1140/epja/i2004-10036-6>
22. FOPI Collaboration, K. Piasecki et al., Wide-acceptance measurement of the K^-/K^+ ratio from Ni+Ni collisions at 1.91A GeV. *Phys. Rev. C* **99**, 014904 (2019). <https://doi.org/10.1103/PhysRevC.99.014904>
23. FOPI Collaboration, M.L. Benabderrahmane et al., Measurement of the In-Medium K^0 Inclusive Cross Section in π^- -Induced Reactions at 1.15GeV/c. *Phys. Rev. Lett.* **102**, 182501 (2009). <https://doi.org/10.1103/PhysRevLett.102.182501>
24. M. Mai, Review of the $\Lambda(1405)$ A curious case of a strangeness resonance. *Eur. Phys. J. Spec. Top.* **230**, 1593–1607 (2021). <https://doi.org/10.1140/epjs/s11734-021-00144-7>
25. T. Sekihara, D. Jido, Y. Kanada-En'yo, $\Lambda(1405)$ -induced non-mesonic decay in kaonic nuclei. *Phys. Rev. C* **79**, 062201 (2009). <https://doi.org/10.1103/PhysRevC.79.062201>
26. E15 Collaboration, T. Yamaga et al., Observation of a $\bar{K}NN$ bound state in the ${}^4\text{He}(K^-, \Lambda p)n$ reaction. *Phys. Rev. C* **102**, 044002 (2020). <https://doi.org/10.1103/PhysRevC.102.044002>
27. T. Yamazaki, Y. Akaishi, (K^-, π^-) production of nuclear \bar{K} bound states in proton-rich systems via Λ^* doorways. *Phys. Lett. B* **535**, 70–76 (2002). [https://doi.org/10.1016/S0370-2693\(02\)01738-0](https://doi.org/10.1016/S0370-2693(02)01738-0)
28. N. Shevchenko, A. Gal, J. Mareš, Faddeev calculation of a K^-pp quasibound state. *Phys. Rev. Lett.* **98**, 082301 (2007). <https://doi.org/10.1103/PhysRevLett.98.082301>
29. N.V. Shevchenko, A. Gal, J. Mareš, J. Révai, $\bar{K}NN$ quasibound state and the $\bar{K}N$ interaction: coupled-channels Faddeev calculations of the $\bar{K}NN-\pi\Sigma N$ system. *Phys. Rev. C* **76**, 044004 (2007). <https://doi.org/10.1103/PhysRevC.76.044004>
30. Y. Ikeda, T. Sato, Strange dibaryon resonance in the $\bar{K}NN-\pi YN$ system. *Phys. Rev. C* **76**, 035203 (2007). <https://doi.org/10.1103/PhysRevC.76.035203>
31. A. Dote, T. Hyodo, W. Weise, K^-pp system with chiral SU(3) effective interaction. *Nucl. Phys. A* **804**, 197–206 (2008). <https://doi.org/10.1016/j.nuclphysa.2008.02.001>
32. Y. Ikeda, T. Sato, Resonance energy of the $\bar{K}NN-\pi YN$ system. *Phys. Rev. C* **79**, 035201 (2009). <https://doi.org/10.1103/PhysRevC.79.035201>
33. S. Wycech, A.M. Green, Variational calculations for \bar{K} -few-nucleon systems. *Phys. Rev. C* **79**, 014001 (2009). <https://doi.org/10.1103/PhysRevC.79.014001>
34. T. Koike, T. Harada, The $\bar{K}N \rightarrow \pi\Sigma$ decay threshold effect in ${}^3\text{He}(\text{in-flight } K^-, n)$ reaction spectrum. *Hyperfine Interact.* **193**, 221–227 (2009). <https://doi.org/10.1007/s10751-009-0004-y>
35. Y. Ikeda, H. Kamano, T. Sato, Energy dependence of $\bar{K}N$ interactions and resonance pole of strange dibaryons. *Prog. Theor. Phys.* **124**, 533–539 (2010). <https://doi.org/10.1143/PTP.124.533>
36. N. Barnea, A. Gal, E. Liverts, Realistic calculations of $\bar{K}NN$, $\bar{K}NNN$, and $\bar{K}\bar{K}NN$ quasibound states. *Phys. Lett. B* **712**, 132–137 (2012). <https://doi.org/10.1016/j.physletb.2012.04.055>

37. M. Bayar, E. Oset, $\bar{K}NN$ absorption within the framework of the fixed-center approximation to Faddeev equations. *Phys. Rev. C* **88**, 044003 (2013). <https://doi.org/10.1103/PhysRevC.88.044003>
38. J. Révai, N. Shevchenko, Faddeev calculations of the $\bar{K}NN$ system with a chirally motivated $\bar{K}N$ interaction. II. The K^-pp quasibound state. *Phys. Rev. C* **90**, 034004 (2014). <https://doi.org/10.1103/PhysRevC.90.034004>
39. A. Doté, T. Inoue, T. Myo, Application of a coupled-channel complex scaling method with Feshbach projection to the K^-pp system. *Prog. Theor. Exp. Phys.* **2015**, 043D02 (2015). <https://doi.org/10.1093/ptep/ptv039>
40. T. Sekihara, E. Oset, A. Ramos, On the structure observed in the in-flight $^3\text{He} (K^-, \Delta p) n$ reaction at J-PARC. *Prog. Theor. Exp. Phys.* **2016**, 123D03 (2016). <https://doi.org/10.1093/ptep/ptw166>
41. S. Ohnishi et al., Few-body approach to the structure of \bar{K} -nuclear quasibound states. *Phys. Rev. C* **95**, 065202 (2017). <https://doi.org/10.1103/PhysRevC.95.065202>
42. A. Doté, T. Inoue, T. Myo, Fully coupled-channels complex scaling method for the K^-pp system. *Phys. Rev. C* **95**, 062201 (2017). <https://doi.org/10.1103/PhysRevC.95.062201>
43. H.-W. Hammer, A. Nogga, A. Schwenk, Colloquium: three-body forces: from cold atoms to nuclei. *Rev. Mod. Phys.* **85**, 197–217 (2013). <https://doi.org/10.1103/RevModPhys.85.197>
44. L.E. Marcucci et al., The hyperspherical harmonics method: a tool for testing and improving nuclear interaction models. *Front. Phys.* **8**, 69 (2020). <https://doi.org/10.3389/fphy.2020.00069>
45. L. Fabbietti, V.M. Sarti, O.V. Doce, Study of the strong interaction among hadrons with correlations at the LHC. *Ann. Rev. Nucl. Part. Sci.* **71**, 377–402 (2021). <https://doi.org/10.1146/annurev-nucl-102419-034438>. [arXiv:2012.09806](https://arxiv.org/abs/2012.09806) [nucl-ex]
46. ALICE Collaboration, S. Acharya et al., $p-p$, $p-\Lambda$ and $\Lambda-\Lambda$ correlations studied via femtoscopy in pp reactions at $\sqrt{s} = 7$ TeV. *Phys. Rev. C* **99**, 024001 (2019). <https://doi.org/10.1103/PhysRevC.99.024001>. [arXiv:1805.12455](https://arxiv.org/abs/1805.12455) [nucl-ex]
47. ALICE Collaboration, S. Acharya et al., Scattering studies with low-energy kaon-proton femtoscopy in proton-proton collisions at the LHC. *Phys. Rev. Lett.* **124**, 092301 (2020). <https://doi.org/10.1103/PhysRevLett.124.092301>. [arXiv:1905.13470](https://arxiv.org/abs/1905.13470) [nucl-ex]
48. ALICE Collaboration, S. Acharya et al., Investigation of the $p-\Sigma^0$ interaction via femtoscopy in pp collisions. *Phys. Lett. B* **805**, 135419 (2020). <https://doi.org/10.1016/j.physletb.2020.135419>. [arXiv:1910.14407](https://arxiv.org/abs/1910.14407)
49. ALICE Collaboration, S. Acharya et al., Study of the $\Lambda-\Lambda$ interaction with femtoscopy correlations in pp and $p\text{-Pb}$ collisions at the LHC. *Phys. Lett. B* **797**, 134822 (2019). <https://doi.org/10.1016/j.physletb.2019.134822>. [arXiv:1905.07209](https://arxiv.org/abs/1905.07209) [nucl-ex]
50. ALICE Collaboration, S. Acharya et al., First observation of an attractive interaction between a proton and a cascade baryon. *Phys. Rev. Lett.* **123**, 112002 (2019). <https://doi.org/10.1103/PhysRevLett.123.112002>. [arXiv:1904.12198](https://arxiv.org/abs/1904.12198) [nucl-ex]
51. ALICE Collaboration, S. Acharya et al., Unveiling the strong interaction among hadrons at the LHC. *Nature* **588**, 232–238 (2020). <https://doi.org/10.1038/s41586-020-3001-6>. [arXiv:2005.11495](https://arxiv.org/abs/2005.11495)
52. ALICE Collaboration, S. Acharya et al., Experimental evidence for an attractive $p-\phi$ interaction. *Phys. Rev. Lett.* **127**, 172301 (2021). <https://doi.org/10.1103/PhysRevLett.127.172301>. [arXiv:2105.05578](https://arxiv.org/abs/2105.05578) [nucl-ex]
53. ALICE Collaboration, S. Acharya et al., Investigating the role of strangeness in baryon-antibaryon annihilation at the LHC. *Phys. Lett. B* **829**, 137060 (2022). <https://doi.org/10.1016/j.physletb.2022.137060>. [arXiv:2105.05190](https://arxiv.org/abs/2105.05190) [nucl-ex]
54. ALICE Collaboration, Constraining the $\bar{K}N$ coupled channel dynamics using femtosopic correlations at the LHC. *Eur. Phys. J. C* **83**(4), 340 (2023). <https://doi.org/10.1140/epjc/s10052-023-11476-0>. [arXiv:2205.15176](https://arxiv.org/abs/2205.15176) [nucl-ex]
55. ALICE Collaboration, S. Acharya et al., Exploring the $N\Lambda$ - $N\Sigma$ coupled system with high precision correlation techniques at the LHC. *Phys. Lett. B* **833**, 137272 (2022). <https://doi.org/10.1016/j.physletb.2022.137272>
56. ALICE Collaboration, First measurement of the Λ - Ξ interaction in proton-proton collisions at the LHC. *Phys. Lett. B* **844**, 137223 (2023). <https://doi.org/10.1016/j.physletb.2022.137223>. [arXiv:2204.10258](https://arxiv.org/abs/2204.10258) [nucl-ex]
57. ALICE Collaboration, S. Acharya et al., First study of the two-body scattering involving charm hadrons. *Phys. Rev. D* **106**, 052010 (2022). <https://doi.org/10.1103/PhysRevD.106.052010>
58. E. Chizzali et al., Evidence of a $p-\phi$ bound state. [arXiv:2212.12690](https://arxiv.org/abs/2212.12690) [nucl-ex]
59. ALICE Collaboration, Towards the understanding of the genuine three-body interaction for $p-p-p$ and $p-p-\Lambda$. *Eur. Phys. J. A* **59**(7), 145 (2023). <https://doi.org/10.1140/epja/s10050-023-00998-6>. [arXiv:2206.03344](https://arxiv.org/abs/2206.03344) [nucl-ex]
60. R. Kubo, Generalized cumulant expansion method. *J. Phys. Soc. Jpn.* **17**, 1100–1120 (1962). <https://doi.org/10.1143/JPSJ.17.1100>
61. R. Del Grande et al., A method to remove lower order contributions in multi-particle femtosopic correlation functions. *Eur. Phys. J. C* **82**, 244 (2022). <https://doi.org/10.1140/epjc/s10052-022-10209-z>. [arXiv:2107.10227](https://arxiv.org/abs/2107.10227) [nucl-th]
62. ALICE Collaboration, K. Aamodt et al., The ALICE experiment at the CERN LHC. *J. Instr.* **3**, S08002 (2008). <https://doi.org/10.1088/1748-0221/3/08/S08002>
63. ALICE Collaboration, B. Abelev et al., Performance of the ALICE experiment at the CERN LHC. *Int. J. Mod. Phys. A* **29**, 1430044 (2014). <https://doi.org/10.1142/S0217751X14300440>
64. ALICE Collaboration, The ALICE experiment—a journey through QCD. [arXiv:2211.04384](https://arxiv.org/abs/2211.04384) [nucl-ex]
65. ALICE Collaboration, E. Abbas et al., “Performance of the ALICE VZERO system”. *JINST* **8**, P10016 (2013). <https://doi.org/10.1088/1748-0221/8/10/P10016>. [arXiv:1306.3130](https://arxiv.org/abs/1306.3130) [nucl-ex]
66. ALICE Collaboration, K. Aamodt et al., Alignment of the ALICE inner tracking system with cosmic-ray tracks. *JINST* **5**, P03003 (2010). <https://doi.org/10.1088/1748-0221/5/03/P03003>. [arXiv:1001.0502](https://arxiv.org/abs/1001.0502) [physics.ins-det]
67. J. Alme et al., The ALICE TPC, a large 3-dimensional tracking device with fast readout for ultra-high multiplicity events. *Nucl. Instrum. Methods A* **622**, 316–367 (2010). <https://doi.org/10.1016/j.nima.2010.04.042>
68. A. Akimov et al., Performance of the ALICE time-of-flight detector at the LHC. *Eur. Phys. J. Plus* **128**, 44 (2013). <https://doi.org/10.1140/epjp/i2013-13044-x>
69. T. Sjöstrand et al., An introduction to PYTHIA 8.2. *Comput. Phys. Commun.* **191**, 159–177 (2015). <https://doi.org/10.1016/j.cpc.2015.01.024>. [arXiv:1410.3012](https://arxiv.org/abs/1410.3012) [hep-ph]
70. GEANT4 Collaboration, S. Agostinelli et al., GEANT4: a simulation toolkit. *Nucl. Instrum. Methods A* **506**, 250–303 (2003). [https://doi.org/10.1016/S0168-9002\(03\)01368-8](https://doi.org/10.1016/S0168-9002(03)01368-8)
71. V. Uzhinsky et al., Antinucleus-nucleus cross sections implemented in Geant4. *Phys. Lett. B* **705**, 235–239 (2011). <https://doi.org/10.1016/j.physletb.2011.10.010>
72. ALICE Collaboration, B.B. Abelev et al., Two- and three-pion quantum statistics correlations in $Pb-Pb$ collisions at $\sqrt{s_{NN}} = 2.76$ TeV at the CERN Large Hadron Collider. *Phys. Rev. C* **89**, 024911 (2014). <https://doi.org/10.1103/PhysRevC.89.024911>. [arXiv:1310.7808](https://arxiv.org/abs/1310.7808) [nucl-ex]
73. R. Lednický, Correlation femtoscopy of multiparticle processes. *Phys. At. Nucl.* **67**, 72–82 (2004). <https://doi.org/10.1134/1.1644010>
74. M.A. Lisa et al., Femtoscopy in relativistic heavy ion collisions. *Ann. Rev. Nucl. Part. Sci.* **55**, 357–402 (2005). <https://doi.org/10.1146/annurev.nucl.55.090704.151533>. [arXiv:nucl-ex/0505014](https://arxiv.org/abs/nucl-ex/0505014)

ALICE Collaboration

S. Acharya¹²⁵, D. Adamová⁸⁶, A. Adler⁶⁹, G. Aglieri Rinella³², M. Agnello²⁹, N. Agrawal⁵⁰, Z. Ahammed¹³², S. Ahmad¹⁵, S. U. Ahn⁷⁰, I. Ahuja³⁷, A. Akimov¹⁴⁰, M. Al-Turany⁹⁷, D. Aleksandrov¹⁴⁰, B. Alessandro⁵⁵, H. M. Alfanda⁶, R. Alfaro Molina⁶⁶, B. Ali¹⁵, A. Alici²⁵, N. Alizadehvandchali¹¹⁴, A. Alkin³², J. Alme²⁰, G. Alocco⁵¹, T. Alt⁶³, I. Altsybeev¹⁴⁰, M. N. Anaam⁶, C. Andrei⁴⁵, A. Andronic¹³⁵, V. Anguelov⁹⁴, F. Antinori⁵³, P. Antonioli⁵⁰, N. Apadula⁷⁴, L. Aphecetche¹⁰³, H. Appelshäuser⁶³, C. Arata⁷³, S. Arcelli²⁵, M. Aresti⁵¹, R. Arnaldi⁵⁵, J. G. M. C. A. Arneiro¹¹⁰, I. C. Arsene¹⁹, M. Arslandok¹³⁷, A. Augustinus³², R. Averbeck⁹⁷, M. D. Azmi¹⁵, A. Badalà⁵², J. Bae¹⁰⁴, Y. W. Baek⁴⁰, X. Bai¹¹⁸, R. Bailhache⁶³, Y. Bailung⁴⁷, A. Balbino²⁹, A. Baldisseri¹²⁸, B. Balis², D. Banerjee⁴, Z. Banoo⁹¹, R. Barbera²⁶, F. Barile³¹, L. Barioglio⁹⁵, M. Barlou⁷⁸, G. G. Barnaföldi¹³⁶, L. S. Barnby⁸⁵, V. Barret¹²⁵, L. Barreto¹¹⁰, C. Bartels¹¹⁷, K. Barth³², E. Bartsch⁶³, N. Bastid¹²⁵, S. Basu⁷⁵, G. Batigne¹⁰³, D. Battistini⁹⁵, B. Batyunya¹⁴¹, D. Bauri⁴⁶, J. L. Bazo Alba¹⁰¹, I. G. Bearden⁸³, C. Beattie¹³⁷, P. Becht⁹⁷, D. Behera⁴⁷, I. Belikov¹²⁷, A. D. C. Bell Hechavarria¹³⁵, F. Bellini²⁵, R. Bellwied¹¹⁴, S. Belokurova¹⁴⁰, G. Bencedi¹³⁶, S. Beole²⁴, A. Bercuci⁴⁵, Y. Berdnikov¹⁴⁰, A. Berdnikova⁹⁴, L. Bergmann⁹⁴, M. G. Besoiu⁶², L. Betev³², P. P. Bhaduri¹³², A. Bhasin⁹¹, M. A. Bhat⁴, B. Bhattacharjee⁴¹, L. Bianchi²⁴, N. Bianchi⁴⁸, J. Bielčák³⁵, J. Bielčíková⁸⁶, J. Biernat¹⁰⁷, A. P. Bigot¹²⁷, A. Bilandzic⁹⁵, G. Biro¹³⁶, S. Biswas⁴, N. Bize¹⁰³, J. T. Blair¹⁰⁸, D. Blau¹⁴⁰, M. B. Blidaru⁹⁷, N. Bluhme³⁸, C. Blume⁶³, G. Boca^{21,54}, F. Bock⁸⁷, T. Bodova²⁰, A. Bogdanov¹⁴⁰, S. Boi²², J. Bok⁵⁷, L. Boldizsár¹³⁶, M. Bombara³⁷, P. M. Bond³², G. Bonomi^{54,131}, H. Borel¹²⁸, A. Borisso¹⁴⁰, A. G. Borquez Carcamo⁹⁴, H. Bossi¹³⁷, E. Botta²⁴, Y. E. M. Bouziani⁶³, L. Bratrud⁶³, P. Braun-Munzinger⁹⁷, M. Bregant¹¹⁰, M. Broz³⁵, G. E. Bruno^{31,96}, M. D. Buckland²³, D. Budnikov¹⁴⁰, H. Buesching⁶³, S. Bufalino²⁹, P. Buhler¹⁰², Z. Buthelezi^{67,121}, A. Bylinkin²⁰, S. A. Bysiak¹⁰⁷, M. Cai⁶, H. Caines¹³⁷, A. Caliva²⁸, E. Calvo Villar¹⁰¹, J. M. M. Camacho¹⁰⁹, P. Camerini²³, F. D. M. Canedo¹¹⁰, M. Carabas¹²⁴, A. A. Carballo³², F. Carnesecchi³², R. Caron¹²⁶, L. A. D. Carvalho¹¹⁰, J. Castillo Castellanos¹²⁸, F. Catalano^{24,32}, C. Ceballos Sanchez¹⁴¹, I. Chakaberia⁷⁴, P. Chakraborty⁴⁶, S. Chandra¹³², S. Chapeland³², M. Chartier¹¹⁷, S. Chattopadhyay¹³², S. Chattopadhyay⁹⁹, T. G. Chavez⁴⁴, T. Cheng^{6,97}, C. Cheshkov¹²⁶, B. Cheynis¹²⁶, V. Chibante Barroso³², D. D. Chinellato¹¹¹, E. S. Chizzali^{95,a}, J. Cho⁵⁷, S. Cho⁵⁷, P. Chochula³², P. Christakoglou⁸⁴, C. H. Christensen⁸³, P. Christiansen⁷⁵, T. Chujo¹²³, M. Ciaccio²⁹, C. Cicalo⁵¹, F. Cindolo⁵⁰, M. R. Ciupek⁹⁷, G. Clai^{50,b}, F. Colamaria⁴⁹, J. S. Colburn¹⁰⁰, D. Colella^{31,96}, M. Colocci²⁵, G. Conesa Balbastre⁷³, Z. Conesa del Valle⁷², G. Contin²³, J. G. Contreras³⁵, M. L. Coquet¹²⁸, T. M. Cormier^{87,*}, P. Cortese^{55,130}, M. R. Cosentino¹¹², F. Costa³², S. Costanza^{21,54}, C. Cot⁷², J. Crkovská⁹⁴, P. Crochet¹²⁵, R. Cruz-Torres⁷⁴, P. Cui⁶, A. Dainese⁵³, M. C. Danisch⁹⁴, A. Danu⁶², P. Das⁸⁰, P. Das⁴, S. Das⁴, A. R. Dash¹³⁵, S. Dash⁴⁶, A. De Caro²⁸, G. de Cataldo⁴⁹, J. de Cuveland³⁸, A. De Falco²², D. De Gruttola²⁸, N. De Marco⁵⁵, C. De Martin²³, S. De Pasquale²⁸, R. Deb¹³¹, S. Deb⁴⁷, K. R. Deja¹³³, R. Del Grande⁹⁵, L. Dello Stritto²⁸, W. Deng⁶, P. Dhankher¹⁸, D. Di Bari³¹, A. Di Mauro³², B. Diab¹²⁸, R. A. Diaz^{7,141}, T. Dietel¹¹³, Y. Ding⁶, R. Divià³², D. U. Dixit¹⁸, Ø. Djuvsland²⁰, U. Dmitrieva¹⁴⁰, A. Dobrin⁶², B. Dönigus⁶³, J. M. Dubinski¹³³, A. Dubla⁹⁷, S. Dudi⁹⁰, P. Dupieux¹²⁵, M. Durkac¹⁰⁶, N. Dzalaiova¹², T. M. Eder¹³⁵, R. J. Ehlers⁷⁴, F. Eisenhut⁶³, D. Elia⁴⁹, B. Erazmus¹⁰³, F. Ercolessi²⁵, F. Erhardt⁸⁹, M. R. Ersdal²⁰, B. Espagnon⁷², G. Eulisse³², D. Evans¹⁰⁰, S. Evdokimov¹⁴⁰, L. Fabbietti⁹⁵, M. Faggin²⁷, J. Faivre⁷³, F. Fan⁶, W. Fan⁷⁴, A. Fantoni⁴⁸, M. Fasel⁸⁷, P. Fedichio²⁹, A. Feliciello⁵⁵, G. Feofilov¹⁴⁰, A. Fernández Téllez⁴⁴, L. Ferrandi¹¹⁰, M. B. Ferrer³², A. Ferrero¹²⁸, C. Ferrero⁵⁵, A. Ferretti²⁴, V. J. G. Feuillard⁹⁴, V. Filova³⁵, D. Finogeev¹⁴⁰, F. M. Fionda⁵¹, F. Flor¹¹⁴, A. N. Flores¹⁰⁸, S. Foertsch⁶⁷, I. Fokin⁹⁴, S. Fokin¹⁴⁰, E. Fragaicomio⁵⁶, E. Frajna¹³⁶, U. Fuchs³², N. Funicello²⁸, C. Furget⁷³, A. Furs¹⁴⁰, T. Fusayasu⁹⁸, J. J. Gaardhøje⁸³, M. Gagliardi²⁴, A. M. Gago¹⁰¹, C. D. Galvan¹⁰⁹, D. R. Gangadharan¹¹⁴, P. Ganoti⁷⁸, C. Garabatos⁹⁷, J. R. A. Garcia⁴⁴, E. Garcia-Solis⁹, C. Gargiulo³², A. Garibli⁸¹, K. Garner¹³⁵, P. Gasik⁹⁷, A. Gautam¹¹⁶, M. B. Gay Ducati⁶⁵, M. Germain¹⁰³, A. Ghimouz¹²³, C. Ghosh¹³², M. Giacalone^{25,50}, P. Giubellino^{55,97}, P. Giubilato²⁷, A. M. C. Glaenger¹²⁸, P. Glässel⁹⁴, E. Glimos¹²⁰, D. J. Q. Goh⁷⁶, V. Gonzalez¹³⁴, S. Gorbunov³⁸, M. Gorgon², K. Goswami⁴⁷, S. Gotovac³³, V. Grabski⁶⁶, L. K. Graczykowski¹³³, E. Grecka⁸⁶, A. Grelli⁵⁸, C. Grigoras³², V. Grigoriev¹⁴⁰, S. Grigoryan^{1,141}, F. Grosa³², J. F. Grosse-Oetringhaus³², R. Grosso⁹⁷, D. Grund³⁵, G. G. Guardiano¹¹¹, R. Guernane⁷³, M. Guilbaud¹⁰³, K. Gulbrandsen⁸³, T. Gundem⁶³, T. Gunji¹²², W. Guo⁶, A. Gupta⁹¹, R. Gupta⁹¹, R. Gupta⁴⁷, S. P. Guzman⁴⁴, K. Gwizdzial¹³³, L. Gyulai¹³⁶, M. K. Habib⁹⁷, C. Hadjidakis⁷², F. U. Haider⁹¹, H. Hamagaki⁷⁶, A. Hamdi⁷⁴, M. Hamid⁶, Y. Han¹³⁸

B. G. Hanley¹³⁴, R. Hannigan¹⁰⁸, J. Hansen⁷⁵, M. R. Haque¹³³, J. W. Harris¹³⁷, A. Harton⁹, H. Hassan⁸⁷, D. Hatzifotiadou⁵⁰, P. Hauer⁴², L. B. Havener¹³⁷, S. T. Heckel⁹⁵, E. Hellbär⁹⁷, H. Helstrup³⁴, M. Hemmer⁶³, T. Herman³⁵, G. Herrera Corral⁸, F. Herrmann¹³⁵, S. Herrmann¹²⁶, K. F. Hetland³⁴, B. Heybeck⁶³, H. Hillemanns³², B. Hippolyte¹²⁷, F. W. Hoffmann⁶⁹, B. Hofman⁵⁸, B. Hohlweger⁸⁴, G. H. Hong¹³⁸, M. Horst⁹⁵, A. Horzyk², Y. Hou⁶, P. Hristov³², C. Hughes¹²⁰, P. Huhn⁶³, L. M. Huhta¹¹⁵, T. J. Humanic⁸⁸, A. Hutson¹¹⁴, D. Hutter³⁸, R. Ilkaev¹⁴⁰, H. Ilyas¹³, M. Inaba¹²³, G. M. Innocenti³², M. Ippolitov¹⁴⁰, A. Isakov⁸⁶, T. Isidori¹¹⁶, M. S. Islam⁹⁹, M. Ivanov¹², M. Ivanov⁹⁷, V. Ivanov¹⁴⁰, K. E. Iversen⁷⁵, M. Jablonski², B. Jacak⁷⁴, N. Jacazio²⁵, P. M. Jacobs⁷⁴, S. Jadlovska¹⁰⁶, J. Jadlovska¹⁰⁶, S. Jaelani⁸², C. Jahnke¹¹¹, M. J. Jakubowska¹³³, M. A. Janik¹³³, T. Janson⁶⁹, M. Jercic⁸⁹, S. Ji¹⁶, S. Jia¹⁰, A. A. P. Jimenez⁶⁴, F. Jonas⁸⁷, J. M. Jowett^{32,97}, J. Jung⁶³, M. Jung⁶³, A. Junique³², A. Jusko¹⁰⁰, M. J. Kabus^{32,133}, J. Kaewjai¹⁰⁵, P. Kalinak⁵⁹, A. S. Kalteyer⁹⁷, A. Kalweit³², V. Kaplin¹⁴⁰, A. Karasu Uysal⁷¹, D. Karatovic⁸⁹, O. Karavichev¹⁴⁰, T. Karavicheva¹⁴⁰, P. Karczmarczyk¹³³, E. Karpechev¹⁴⁰, U. Kebschull⁶⁹, R. Keidel¹³⁹, D. L. D. Keijdener⁵⁸, M. Keil³², B. Ketzer⁴², S. S. Khade⁴⁷, A. M. Khan^{6,118}, S. Khan¹⁵, A. Khanzadeev¹⁴⁰, Y. Kharlov¹⁴⁰, A. Khatun¹¹⁶, A. Khuntia¹⁰⁷, M. B. Kidson¹¹³, B. Kileng³⁴, B. Kim¹⁰⁴, C. Kim¹⁶, D. J. Kim¹¹⁵, E. J. Kim⁶⁸, J. Kim¹³⁸, J. S. Kim⁴⁰, J. Kim⁵⁷, J. Kim⁶⁸, M. Kim¹⁸, S. Kim¹⁷, T. Kim¹³⁸, K. Kimura⁹², S. Kirsch⁶³, I. Kisel³⁸, S. Kiselev¹⁴⁰, A. Kisiel¹³³, J. P. Kitowski², J. L. Klay⁵, J. Klein³², S. Klein⁷⁴, C. Klein-Bösing¹³⁵, M. Kleiner⁶³, T. Klemenz⁹⁵, A. Kluge³², A. G. Knospe¹¹⁴, C. Kobdaj¹⁰⁵, T. Kollegger⁹⁷, A. Kondratyev¹⁴¹, N. Kondratyeva¹⁴⁰, E. Kondratyuk¹⁴⁰, J. König⁶³, S. A. Königstorfer⁹⁵, P. J. Konopka³², G. Kornakov¹³³, S. D. Koryciak², A. Kotliarov⁸⁶, V. Kovalenko¹⁴⁰, M. Kowalski¹⁰⁷, V. Kozuharov³⁶, I. Králik⁵⁹, A. Kravčáková³⁷, L. Krcal^{32,38}, M. Krivda^{59,100}, F. Krizek⁸⁶, K. Krizkova Gajdosova³², M. Kroesen⁹⁴, M. Krüger⁶³, D. M. Krupova³⁵, E. Kryshen¹⁴⁰, V. Kučera⁵⁷, C. Kuhn¹²⁷, P. G. Kuijter⁸⁴, T. Kumaoka¹²³, D. Kumar¹³², L. Kumar⁹⁰, N. Kumar⁹⁰, S. Kumar³¹, S. Kundu³², P. Kurashvili⁷⁹, A. Kurepin¹⁴⁰, A. B. Kurepin¹⁴⁰, A. Kuryakin¹⁴⁰, S. Kushpil⁸⁶, J. Kvapil¹⁰⁰, M. J. Kweon⁵⁷, Y. Kwon¹³⁸, S. L. La Pointe³⁸, P. La Rocca²⁶, A. Lakrathok¹⁰⁵, M. Lamanna³², R. Langoy¹¹⁹, P. Larionov³², E. Laudi³², L. Lautner^{32,95}, R. Lavicka¹⁰², R. Lea^{54,131}, H. Lee¹⁰⁴, I. Legrand⁴⁵, G. Legras¹³⁵, J. Lehrbach³⁸, T. M. Lelek², R. C. Lemmon⁸⁵, I. León Monzón¹⁰⁹, M. M. Lesch⁹⁵, E. D. Lesser¹⁸, P. Lévai¹³⁶, X. Li¹⁰, X. L. Li⁶, J. Lien¹¹⁹, R. Lietava¹⁰⁰, I. Likmeta¹¹⁴, B. Lim²⁴, S. H. Lim¹⁶, V. Lindenstruth³⁸, A. Lindner⁴⁵, C. Lippmann⁹⁷, A. Liu¹⁸, D. H. Liu⁶, J. Liu¹¹⁷, G. S. S. Liveraro¹¹¹, I. M. Lofnes²⁰, C. Loizides⁸⁷, S. Lokos¹⁰⁷, J. Lomker⁵⁸, P. Loncar³³, J. A. Lopez⁹⁴, X. Lopez¹²⁵, E. López Torres⁷, P. Lu^{97,118}, J. R. Luhder¹³⁵, M. Lunardon²⁷, G. Luparello⁵⁶, Y. G. Ma³⁹, M. Mager³², A. Maire¹²⁷, M. V. Makariev³⁶, M. Malaev¹⁴⁰, G. Malfattore²⁵, N. M. Malik⁹¹, Q. W. Malik¹⁹, S. K. Malik⁹¹, L. Malinina^{141,e}, D. Mallick⁸⁰, N. Mallick⁴⁷, G. Mandaglio^{30,52}, S. K. Mandal⁷⁹, V. Manko¹⁴⁰, F. Manso¹²⁵, V. Manzari⁴⁹, Y. Mao⁶, R. W. Marcjan², G. V. Margagliotti²³, A. Margotti⁵⁰, A. Marín⁹⁷, C. Markert¹⁰⁸, P. Martinengo³², M. I. Martínez⁴⁴, G. Martínez García¹⁰³, M. P. P. Martins¹¹⁰, S. Masciocchi⁹⁷, M. Maserà²⁴, A. Masoni⁵¹, L. Massacrier⁷², A. Mastroserio^{49,129}, O. Matonoha⁷⁵, S. Mattiazzo²⁷, P. F. T. Matuoka¹¹⁰, A. Matyja¹⁰⁷, C. Mayer¹⁰⁷, A. L. Mazuecos³², F. Mazzaschi²⁴, M. Mazzilli³², J. E. Mdhului¹²¹, A. F. Mechler⁶³, Y. Melikyan^{43,140}, A. Menchaca-Rocha⁶⁶, E. Meninno^{28,102}, A. S. Menon¹¹⁴, M. Meres¹², S. Mhlanga^{67,113}, Y. Miake¹²³, L. Micheletti³², L. C. Migliorin¹²⁶, D. L. Mihaylov⁹⁵, K. Mikhaylov^{140,141}, A. N. Mishra¹³⁶, D. Miśkowiec⁹⁷, A. Modak⁴, A. P. Mohanty⁵⁸, B. Mohanty⁸⁰, M. Mohisin Khan^{15,c}, M. A. Molander⁴³, Z. Moravcova⁸³, C. Mordasini⁹⁵, D. A. Moreira De Godoy¹³⁵, I. Morozov¹⁴⁰, A. Morsch³², T. Mrnjavac³², V. Muccifora⁴⁸, S. Muhuri¹³², J. D. Mulligan⁷⁴, A. Mulliri²², M. G. Munhoz¹¹⁰, R. H. Munzer⁶³, H. Murakami¹²², S. Murray¹¹³, L. Musa³², J. Musinsky⁵⁹, J. W. Myrcha¹³³, B. Naik¹²¹, A. I. Nambrath¹⁸, B. K. Nandi⁴⁶, R. Nania⁵⁰, E. Nappi⁴⁹, A. F. Nassirpour^{17,75}, A. Nath⁹⁴, C. Nattress¹²⁰, M. N. Naydenov³⁶, A. Neagu¹⁹, A. Negru¹²⁴, L. Nellen⁶⁴, G. Neskovic³⁸, B. S. Nielsen⁸³, E. G. Nielsen⁸³, S. Nikolaev¹⁴⁰, S. Nikulin¹⁴⁰, V. Nikulin¹⁴⁰, F. Noferini⁵⁰, S. Noh¹¹, P. Nomokonov¹⁴¹, J. Norman¹¹⁷, N. Novitzky¹²³, P. Nowakowski¹³³, A. Nyanin¹⁴⁰, J. Nystrand²⁰, M. Ogino⁷⁶, A. Ohlson⁷⁵, V. A. Okorokov¹⁴⁰, J. Oleniacz¹³³, A. C. Oliveira Da Silva¹²⁰, M. H. Oliver¹³⁷, A. Onnerstad¹¹⁵, C. Oppedisano⁵⁵, A. Ortiz Velasquez⁶⁴, J. Otwinowski¹⁰⁷, M. Oya⁹², K. Oyama⁷⁶, Y. Pachmayer⁹⁴, S. Padhan⁴⁶, D. Pagano^{54,131}, G. Paic⁶⁴, A. Palasciano⁴⁹, S. Panebianco¹²⁸, H. Park¹²³, H. Park¹⁰⁴, J. Park⁵⁷, J. E. Parkkila³², R. N. Patra⁹¹, B. Paul²², H. Pei⁶, T. Peitzmann⁵⁸, X. Peng⁶, M. Pennisi²⁴, D. Peresunko¹⁴⁰, G. M. Perez⁷, S. Perrin¹²⁸, Y. Pestov¹⁴⁰, V. Petrov¹⁴⁰, M. Petrovici⁴⁵, R. P. Pezzi^{65,103}, S. Piano⁵⁶, M. Pikna¹², P. Pillot¹⁰³, O. Pinazza^{32,50}, L. Pinsky¹¹⁴, C. Pinto⁹⁵, S. Pisano⁴⁸, M. Płoskoń⁷⁴, M. Planinic⁸⁹, F. Pliquet⁶³, M. G. Poghosyan⁸⁷, B. Polichtchouk¹⁴⁰, S. Politano²⁹

- ³ Bogolyubov Institute for Theoretical Physics, National Academy of Sciences of Ukraine, Kiev, Ukraine
- ⁴ Department of Physics, Bose Institute, Centre for Astroparticle Physics and Space Science (CAPSS), Kolkata, India
- ⁵ California Polytechnic State University, San Luis Obispo, CA, USA
- ⁶ Central China Normal University, Wuhan, China
- ⁷ Centro de Aplicaciones Tecnológicas y Desarrollo Nuclear (CEADEN), Havana, Cuba
- ⁸ Centro de Investigación y de Estudios Avanzados (CINVESTAV), Mérida and Mexico City, Mexico
- ⁹ Chicago State University, Chicago, IL, USA
- ¹⁰ China Institute of Atomic Energy, Beijing, China
- ¹¹ Chungbuk National University, Cheongju, Republic of Korea
- ¹² Faculty of Mathematics, Physics and Informatics, Comenius University Bratislava, Bratislava, Slovak Republic
- ¹³ COMSATS University Islamabad, Islamabad, Pakistan
- ¹⁴ Creighton University, Omaha, NE, USA
- ¹⁵ Department of Physics, Aligarh Muslim University, Aligarh, India
- ¹⁶ Department of Physics, Pusan National University, Pusan, Republic of Korea
- ¹⁷ Department of Physics, Sejong University, Seoul, Republic of Korea
- ¹⁸ Department of Physics, University of California, Berkeley, CA, USA
- ¹⁹ Department of Physics, University of Oslo, Oslo, Norway
- ²⁰ Department of Physics and Technology, University of Bergen, Bergen, Norway
- ²¹ Dipartimento di Fisica, Università di Pavia, Pavia, Italy
- ²² Dipartimento di Fisica dell'Università and Sezione INFN, Cagliari, Italy
- ²³ Dipartimento di Fisica dell'Università and Sezione INFN, Trieste, Italy
- ²⁴ Dipartimento di Fisica dell'Università and Sezione INFN, Turin, Italy
- ²⁵ Dipartimento di Fisica e Astronomia dell'Università and Sezione INFN, Bologna, Italy
- ²⁶ Dipartimento di Fisica e Astronomia dell'Università and Sezione INFN, Catania, Italy
- ²⁷ Dipartimento di Fisica e Astronomia dell'Università and Sezione INFN, Padua, Italy
- ²⁸ Dipartimento di Fisica 'E.R. Caianiello' dell'Università and Gruppo Collegato INFN, Salerno, Italy
- ²⁹ Dipartimento DISAT del Politecnico and Sezione INFN, Turin, Italy
- ³⁰ Dipartimento di Scienze MIFT, Università di Messina, Messina, Italy
- ³¹ Dipartimento Interateneo di Fisica 'M. Merlin' and Sezione INFN, Bari, Italy
- ³² European Organization for Nuclear Research (CERN), Geneva, Switzerland
- ³³ Faculty of Electrical Engineering, Mechanical Engineering and Naval Architecture, University of Split, Split, Croatia
- ³⁴ Faculty of Engineering and Science, Western Norway University of Applied Sciences, Bergen, Norway
- ³⁵ Faculty of Nuclear Sciences and Physical Engineering, Czech Technical University in Prague, Prague, Czech Republic
- ³⁶ Faculty of Physics, Sofia University, Sofia, Bulgaria
- ³⁷ Faculty of Science, P.J. Šafárik University, Kosice, Slovak Republic
- ³⁸ Frankfurt Institute for Advanced Studies, Johann Wolfgang Goethe-Universität Frankfurt, Frankfurt, Germany
- ³⁹ Fudan University, Shanghai, China
- ⁴⁰ Gangneung-Wonju National University, Gangneung, Republic of Korea
- ⁴¹ Gauhati University, Department of Physics, Guwahati, India
- ⁴² Helmholtz-Institut für Strahlen- und Kernphysik, Rheinische Friedrich-Wilhelms-Universität Bonn, Bonn, Germany
- ⁴³ Helsinki Institute of Physics (HIP), Helsinki, Finland
- ⁴⁴ High Energy Physics Group, Universidad Autónoma de Puebla, Puebla, Mexico
- ⁴⁵ Horia Hulubei National Institute of Physics and Nuclear Engineering, Bucharest, Romania
- ⁴⁶ Indian Institute of Technology Bombay (IIT), Mumbai, India
- ⁴⁷ Indian Institute of Technology Indore, Indore, India
- ⁴⁸ INFN, Laboratori Nazionali di Frascati, Frascati, Italy
- ⁴⁹ INFN, Sezione di Bari, Bari, Italy
- ⁵⁰ INFN, Sezione di Bologna, Bologna, Italy
- ⁵¹ INFN, Sezione di Cagliari, Cagliari, Italy
- ⁵² INFN, Sezione di Catania, Catania, Italy
- ⁵³ INFN, Sezione di Padova, Padua, Italy
- ⁵⁴ INFN, Sezione di Pavia, Pavia, Italy
- ⁵⁵ INFN, Sezione di Torino, Turin, Italy

- ⁵⁶ INFN, Sezione di Trieste, Trieste, Italy
- ⁵⁷ Inha University, Incheon, Republic of Korea
- ⁵⁸ Institute for Gravitational and Subatomic Physics (GRASP), Utrecht University/Nikhef, Utrecht, The Netherlands
- ⁵⁹ Institute of Experimental Physics, Slovak Academy of Sciences, Kosice, Slovak Republic
- ⁶⁰ Institute of Physics, Homi Bhabha National Institute, Bhubaneswar, India
- ⁶¹ Institute of Physics of the Czech Academy of Sciences, Prague, Czech Republic
- ⁶² Institute of Space Science (ISS), Bucharest, Romania
- ⁶³ Institut für Kernphysik, Johann Wolfgang Goethe-Universität Frankfurt, Frankfurt, Germany
- ⁶⁴ Instituto de Ciencias Nucleares, Universidad Nacional Autónoma de México, Mexico City, Mexico
- ⁶⁵ Instituto de Física, Universidade Federal do Rio Grande do Sul (UFRGS), Porto Alegre, Brazil
- ⁶⁶ Universidad Nacional Autónoma de México, Instituto de Física, Mexico City, Mexico
- ⁶⁷ iThemba LABS, National Research Foundation, Somerset West, South Africa
- ⁶⁸ Jeonbuk National University, Jeonju, Republic of Korea
- ⁶⁹ Johann-Wolfgang-Goethe Universität Frankfurt Institut für Informatik, Fachbereich Informatik und Mathematik, Frankfurt, Germany
- ⁷⁰ Korea Institute of Science and Technology Information, Daejeon, Republic of Korea
- ⁷¹ KTO Karatay University, Konya, Turkey
- ⁷² Laboratoire de Physique des 2 Infinis, Irène Joliot-Curie, Orsay, France
- ⁷³ Laboratoire de Physique Subatomique et de Cosmologie, Université Grenoble-Alpes, CNRS-IN2P3, Grenoble, France
- ⁷⁴ Lawrence Berkeley National Laboratory, Berkeley, CA, USA
- ⁷⁵ Division of Particle Physics, Department of Physics, Lund University, Lund, Sweden
- ⁷⁶ Nagasaki Institute of Applied Science, Nagasaki, Japan
- ⁷⁷ Nara Women's University (NWU), Nara, Japan
- ⁷⁸ Department of Physics, School of Science, National and Kapodistrian University of Athens, Athens, Greece
- ⁷⁹ National Centre for Nuclear Research, Warsaw, Poland
- ⁸⁰ National Institute of Science Education and Research, Homi Bhabha National Institute, Jatni, India
- ⁸¹ National Nuclear Research Center, Baku, Azerbaijan
- ⁸² National Research and Innovation Agency-BRIN, Jakarta, Indonesia
- ⁸³ Niels Bohr Institute, University of Copenhagen, Copenhagen, Denmark
- ⁸⁴ Nikhef, National institute for subatomic physics, Amsterdam, The Netherlands
- ⁸⁵ Nuclear Physics Group, STFC Daresbury Laboratory, Daresbury, UK
- ⁸⁶ Nuclear Physics Institute of the Czech Academy of Sciences, Husinec-Řež, Czech Republic
- ⁸⁷ Oak Ridge National Laboratory, Oak Ridge, TN, USA
- ⁸⁸ Ohio State University, Columbus, OH, USA
- ⁸⁹ Physics Department, Faculty of science, University of Zagreb, Zagreb, Croatia
- ⁹⁰ Physics Department, Panjab University, Chandigarh, India
- ⁹¹ Physics Department, University of Jammu, Jammu, India
- ⁹² Physics Program and International Institute for Sustainability with Knotted Chiral Meta Matter (SKCM2), Hiroshima University, Hiroshima, Japan
- ⁹³ Physikalisches Institut, Eberhard-Karls-Universität Tübingen, Tübingen, Germany
- ⁹⁴ Physikalisches Institut, Ruprecht-Karls-Universität Heidelberg, Heidelberg, Germany
- ⁹⁵ Physik Department, Technische Universität München, Munich, Germany
- ⁹⁶ Politecnico di Bari and Sezione INFN, Bari, Italy
- ⁹⁷ Research Division and ExtreMe Matter Institute EMMI, GSI Helmholtzzentrum für Schwerionenforschung GmbH, Darmstadt, Germany
- ⁹⁸ Saga University, Saga, Japan
- ⁹⁹ Saha Institute of Nuclear Physics, Homi Bhabha National Institute, Kolkata, India
- ¹⁰⁰ School of Physics and Astronomy, University of Birmingham, Birmingham, UK
- ¹⁰¹ Sección Física, Departamento de Ciencias, Pontificia Universidad Católica del Perú, Lima, Peru
- ¹⁰² Stefan Meyer Institut für Subatomare Physik (SMI), Vienna, Austria
- ¹⁰³ SUBATECH, IMT Atlantique, CNRS-IN2P3, Nantes Université, Nantes, France
- ¹⁰⁴ Sungkyunkwan University, Suwon City, Republic of Korea
- ¹⁰⁵ Suranaree University of Technology, Nakhon Ratchasima, Thailand

- 106 Technical University of Košice, Kosice, Slovak Republic
 107 The Henryk Niewodniczanski Institute of Nuclear Physics, Polish Academy of Sciences, Cracow, Poland
 108 The University of Texas at Austin, Austin, TX, USA
 109 Universidad Autónoma de Sinaloa, Culiacán, Mexico
 110 Universidade de São Paulo (USP), São Paulo, Brazil
 111 Universidade Estadual de Campinas (UNICAMP), Campinas, Brazil
 112 Universidade Federal do ABC, Santo Andre, Brazil
 113 University of Cape Town, Cape Town, South Africa
 114 University of Houston, Houston, TX, USA
 115 University of Jyväskylä, Jyväskylä, Finland
 116 University of Kansas, Lawrence, KS, USA
 117 University of Liverpool, Liverpool, UK
 118 University of Science and Technology of China, Hefei, China
 119 University of South-Eastern Norway, Kongsberg, Norway
 120 University of Tennessee, Knoxville, TN, USA
 121 University of the Witwatersrand, Johannesburg, South Africa
 122 University of Tokyo, Tokyo, Japan
 123 University of Tsukuba, Tsukuba, Japan
 124 University Politehnica of Bucharest, Bucharest, Romania
 125 CNRS/IN2P3, LPC, Université Clermont Auvergne, Clermont-Ferrand, France
 126 CNRS/IN2P3, Institut de Physique des 2 Infinis de Lyon, Université de Lyon, Lyon, France
 127 CNRS, IPHC UMR 7178, Université de Strasbourg, 67000 Strasbourg, France
 128 Département de Physique Nucléaire (DPhN), IRFU, Université Paris-Saclay Centre d'Etudes de Saclay (CEA), Saclay, France
 129 Università degli Studi di Foggia, Foggia, Italy
 130 Università del Piemonte Orientale, Vercelli, Italy
 131 Università di Brescia, Brescia, Italy
 132 Variable Energy Cyclotron Centre, Homi Bhabha National Institute, Kolkata, India
 133 Warsaw University of Technology, Warsaw, Poland
 134 Wayne State University, Detroit, MI, USA
 135 Institut für Kernphysik, Westfälische Wilhelms-Universität Münster, Münster, Germany
 136 Wigner Research Centre for Physics, Budapest, Hungary
 137 Yale University, New Haven, CT, USA
 138 Yonsei University, Seoul, Republic of Korea
 139 Zentrum für Technologie und Transfer (ZTT), Worms, Germany
 140 Affiliated with an Institute Covered by a Cooperation Agreement with CERN, Geneva, Switzerland
 141 Affiliated with an International Laboratory Covered by a Cooperation Agreement with CERN, Geneva, Switzerland

^a Also at: Max-Planck-Institut für Physik, Munich, Germany

^b Also at: Italian National Agency for New Technologies, Energy and Sustainable Economic Development (ENEA), Bologna, Italy

^c Also at: Department of Applied Physics, Aligarh Muslim University, Aligarh, India

^d Also at: Institute of Theoretical Physics, University of Wrocław, Wrocław, Poland

^e Also at: An Institution Covered by a Cooperation Agreement with CERN, Geneva, Switzerland

* Deceased